Kidney International, Vol. 67 (2005), pp. 1350–1361

The lipopolysaccharide-triggered mesangial transcriptome: Evaluating the role of interferon regulatory factor-1

YUYANG FU, CHUN XIE, MEI YAN, QUAN LI, JAE WON JOH, CHRISTOPHER LU, and CHANDRA MOHAN

Simmons Arthritis Research Center, Division of Rheumatology, Center for Immunology, University of Texas Southwestern Medical Center, Dallas, Texas; and Department of Nephrology, University of Texas Southwestern Medical Center, Dallas, Texas

The lipopolysaccharide-triggered mesangial transcriptome: Evaluating the role of interferon regulatory factor-1.

Background. Presently, we do not have a clear picture of how the mesangial transcriptome evolves following stimulation. The present study was designed to address this, using an innate trigger to stimulate murine mesangial cells.

Methods. Three independent mesangial cell lines derived from C57BL/6 mice were stimulated with lipopolysaccharide (LPS). The mesangial cell transcriptomes were defined 1, 6, 24, and 60 hours poststimulation with LPS, using a 17,000 gene oligonucleotide array.

Results. Interferon regulatory factor-1 (*IRF-1*), *ScyA2/MCP1*, *ScyA20/MIP3α* (*ScyB1/Gro1*, and *ScyB2/MIP2α/Gro2* were the earliest genes to be hyperexpressed after LPS stimulation. Later-appearing genes included *ScyA7/MCP3*, *ScyD1/fractalkine*, *GM-CSF/CSF-2*, *PDGF, epiregulin, NfKb*, *C/EBP*, *TIMP-1*, *MMP11*, *MMP13*, *PTGS2/COX2*, *SpI2-1*, *Spp1*, *PAI-1*, *VCAM-1, C3*, and *defensin*-β*1*, among others. Several of these changes were validated by real-time polymerase chain reaction (PCR) or enzyme-linked immunosorbent assay (ELISA). Rapid *IRF-1* hyperexpression was also noted following stimulation of mesangial cells with peptidoglycan, poly I:poly C, interferon-γ ?(IFN-γ), and heat-aggregated IgG. However, the blocking of *IRF-1* using RNA interference and the use of mesangial cells isolated from *IRF-1*–deficient mice could not substantiate an obligatory role for *IRF-1* in LPS-induced mesangial cell activation. Likewise, IRF-1 deficiency did not impact the development of anti-glomerular basement membrane (GBM)-induced immune nephritis.

Conclusion. Innate stimuli such as LPS appear to trigger successive waves of mesangial cell gene expression. Although *IRF-1* surfaces as an "early-on, early-off" transcription factor following several different triggers, it does not appear to be an essential molecule for mesangial cell activation by innate triggers or for anti-GBM disease.

The mesangial cell constitutes a key glomerular cell type that plays a potentially important role in the pathogenesis of several renal diseases [1–3]. In particular, it has been recognized to produce a rich array of mediators, including cytokines and chemokines, reactive oxygen species, nitric oxide, prostaglandins, etc. In addition, these cells possess unique contractile properties that allow them to regulate the local blood flow in the glomerulus. Finally, they also elaborate the glomerular basement membrane (GBM) matrix and contribute to the fibrosclerotic lesions seen later in disease, following a variety of primary triggers.

Although a rich literature exists detailing the up-regulation of several different molecules in mesangial cells upon stimulation, little information is currently available concerning the transcriptome of stimulated mesangial cells. This is an important impetus for the current study. In addition, ongoing research in our laboratory implicates genetically encoded differences in the end organs as being potentially important in facilitating the development of immune nephritis [4, 5]. Clearly, it is imperative to define the "normal" mesangial transcriptome in detail before any potential strain or locus specific genetic aberrations can be examined in the future. This is a second factor that has inspired the present study.

A wide variety of stimuli have been documented to trigger mesangial cells, including innate stimuli triggering different Toll receptors, interferon-γ (IFN-γ), interleukin (IL)-1, and other cytokines, and immune complexes [1–3]. This manuscript focuses on mesangial transcriptomic changes following stimulation of Toll-like receptor 4 (TLR4), using lipopolysaccharide (LPS). As a follow-up, this study also tests the functional importance of one of the earliest transcription factors up-regulated following mesangial cell stimulation, interferon regulatory factor-1 (*IRF-1*).

Key words: glomerulonephritis, mesangial, chemokines, lupus, microarray.

Received for publication March 12, 2004
and in revised form July 16, 2004, and September 16, 2004
Accepted for publication October 14, 2004

METHODS

Mesangial cell isolation and stimulation

Three independent mesangial cell lines (labeled B6-M3, B6-M4, and B6-M14) were derived from three 2-month-old C57BL/6 (B6)[3] mice following previously documented protocols [6]. Likewise, mesangial cells were

also prepared from B6.IRF-1$^{-/-}$ mice, purchased from Jackson Laboratories (Bar Harbor, ME, USA). Essentially, renal cortices from the kidneys were minced and then pressed through a series of sieves of decreasing pore size (250 μm mesh, 150 μm, and 75 μm). The glomeruli were collected on the finest sieve (>95% purity, as assessed microscopically), washed with sterile phosphate-buffered saline (PBS), and cultured in Dulbecco's modified Eagle's medium (DMEM) supplemented with nonessential amino acids, 2-mercaptoethanol (2-ME), antibiotics, and 10% horse serum. Importantly, this medium contained D-valine, instead of L-valine, to suppress fibroblast outgrowth. Although these cultures initially possessed other glomerulocyte cell types, notably podocytes, mesangial cells outgrew other cell types after 2 weeks of culture. Flow cytometric analyses of the cultured cells revealed them to be large (based on forward scatter), complex (as ascertained by side scatter) and myosin positive, but negative for keratin, von Willebrand factor, and CD45. All mesangial cells were used between the 10th and 20th passage of cultivation. Cells were plated in serum-free medium and stimulated with LPS at 10 ng/mL. At the indicated time points (0, 1, 6, 24, and 60 hours after LPS stimulation), aliquots of cells were processed for RNA isolation. In other experiments, mesangial cells were stimulated with peptidoglycan (100 ug/mL), poly I:C (100 ug/mL), cytosine phosphate guanosine (CpG) oligonucleotides (10 nmol/L), IL-1β (1 ng/mL), INF-γ (5 ng/mL), or total rabbit IgG (10 ug/mL), purchased from Sigma Chemical Co. (St. Louis, MO, USA). These concentrations were selected based on preliminary dose-response experiments with each individual trigger.

Microarray studies

All protocols used for the microarray studies are detailed at the following Web site: *http://microarraycore.swmed.edu/tech_support.html*. Total RNA was prepared using RNAeasy Mini Kit (Qiagen, Valencia, CA, USA), using manufacturer-suggested protocols. Isolated RNA was amplified once using MessageAmp aRNA kit (Ambion, Woodward, TX, USA), following manufacturer-suggested protocols. We have previously established the relative utility and reliability of using amplified RNA (aRNA) versus unamplified RNA (*http://microarraycore.swmed.edu/*). The aRNA prepared was then labeled with cyanine-3 (Cy3) or cyanine-5 (Cy5), using the ASAP aRNA Labeling Kit (Perkin-Elmer, Wellesley, MA, USA). Both sets of labeled probes were mixed and hybridized to a mouse 17K-oligonucleotide array, consisting of oligonucleotides drawn from the Unigene cluster. The gene content of this array is detailed at the University of Texas Southwestern Medical Center Microarray Core's Web site (*http://microarraycore.swmed.edu/*). Following a series of washes with standard sodium citrate (SSC) and sodium dodecyl sulfate (SDS)-containing buffers, the slides were spin-dried, and scanned using Genepix 4000B. Recorded pixel intensities in the Cy3 and Cy5 fluorescent channels were digitally stored, and analyzed as described below.

Microarray data analysis

The chips were first examined for hybridization quality; isolated subgrids where the hybridization was not satisfactory were flagged and genes from those regions were excluded from further analysis. Although there were 17,000 gene spots on the arrays, about 44% of the spots were flagged away for being unsatisfactory, so that each array yielded only about 9500 data points, on the average. Among the genes that displayed differential expression, the chip-to-chip consistency was good, with the interchip correlation coefficients ranging from 0.35 to 0.78. Fluorescence intensities on all arrays were next subgrid normalized. To remove noise, the mean pixel intensity of each gene was then compared to the local background intensity. Genes that exhibited intensities that were <2 SD above the mean background intensity in >75% of component pixels were excluded from analysis. In addition, genes whose mean fluorescence intensities fell below 1% of the array-wide maximal fluorescence intensity were also excluded.

Of the remaining array spots, those that differed in expression between the control (i.e., unstimulated) and experimental (i.e., LPS-stimulated) by > twofold were examined further. Hierarchic clustering was performed using Gene Traffic (Iobion, La Jolla, CA, USA), based the Pearson correlation distance metric and the "average" clustering algorithm. Statistical significance of any observed expression differences between the unstimulated and stimulated samples were determined using the Student *t* test (Sigmastat) (Jandel Scientific, San Rafael, CA, USA). Since the expression differences failed to maintain significance after multiple testing correction (because of the small number of arrays studied, and the large number of genes being analyzed), the validity of the observed expression differences were confirmed by one of two orthogonal methods, real-time reverse transcription-polymerase chain reaction (RT-PCR) or enzyme-linked immunosorbent assay (ELISA) measurement of corresponding protein levels, for selected genes showing maximal expression differences at the different time points studied. All microarray data detailed in this communication are freely available from the corresponding author.

Potential transcription factor binding sites were identified as follows. The sequence of each differentially expressed gene was accessed on the Ensembl database (*www.ensembl.org*). One thousand base pairs upstream

Table 1. Primer sequences used for real-time reverse transcription-polymerase chain reaction (RT-PCR) studies

Mouse	Gene	Primer sequence
GAPDH	5′	AACGACCCCTTCATTGAC
	3′	TCCACGACATACTCAGCAC
IRF-1	5′	CATTCACACAGGCCGATACAAAGC
	3′	CAACGGAAGTTTGCCTTCCATGTC
GRO1	5′	CCTGAAGCTCCCTTDDTTCAGAAA
	3′	GCCATCAGAGCAGTCTGTCTTCTT
C3	5′	CAGAGCTGGTTGTGGACCATAGAA
	3′	AATCTCCCAGGTGGTGATGGAATC
MMP-13	5′	CTGGTCTGATGTGACACCACTGAA
	3′	CCAGAAGACCAGAAGGTCCATCAA

Abbreviations are: GAPDH, glyceraldehyde-3-phosphate dehydrogenase; IRF-1, interferon regulatory factor-1; GRO1, growth-regulated oncogene 1; C3, complement C3; MMP-13, matrix metalloproteinase-13.

of each gene were selected and tested for transcription factor binding sites using the TESS database (*http://www.cbil.upenn.edu/tess/*). The stringency of comparison was set so that only putative binding sites with >90% match over eight consecutive base pairs, and an L_a/length ratio of 2.0 were considered (where L_a represents the log likelihood score). The respective percentages of all hyperexpressed genes that exhibited the different transcription factor binding sites were then computed.

Real-time RT-PCR studies

Total RNA was isolated from the mesangial cells as described above and quantitated spectrophotometrically. RT-PCR was performed using the enhanced avian horse serum (HS) RT-PCR kit (Sigma Chemical Co.), according to the manufacturer's protocol. Real-time PCR was performed using GeneAmp 5600 (Perkin-Elmer), using primers whose sequences are listed in Table 1. For each pair of primers, PCR was performed over a range of cycles, and the relationship between the quantity of RNA substrate and the final PCR product was defined. Glyceraldehyde-3-phosphate dehydrogenase (*GAPDH*) was assayed in parallel, as an internal control. For both the test message and the *GAPDH* control, the C_T was determined, where C_T refers to the number of PCR cycles required to reach a product intensity threshold. The C_T of each test message was first normalized using the C_T for *GAPDH*, assayed in the same sample. Fold change was next calculated using the relative C_T method, as follows: fold change = $2^{(\text{normalized } C_T \text{ in resting sample} - \text{normalized CT in stimulated sample})}$.

ELISA

Granulocyte macrophage-colony-stimulating factor (GM-CSF), monocyte chemoattractant protein-1 (MCP-1), matrix metalloproteinase-13 (MMP-13), and tissue inhibitors of metalloproteinase-1 (TIMP-1) protein levels were measured using commercially available ELISA kits (R&D Systems, Minneapolis, MN, USA), following manufacturer-suggested protocols. Briefly, Immulon I ELISA plates were first coated with the respective capture antibodies specific for the different chemokines or cytokines. The plates were then blocked overnight with PBS supplemented with 3% bovine serum albumin (BSA), 0.1% gelatin, and 3 mmol/L ethylenediaminetetraacetic acid (EDTA). Supernatant (at 1:2 dilutions), and cytokine/chemokine standards (serial 1:5 dilutions, starting from 1 μg/mL) (R&D Systems), were incubated in duplicate, for 2 hours at room temperature, followed by incubation with alkaline phosphatase (or peroxidase)-conjugated second antibodies specific for the respective cytokines/chemokines. The plates were finally developed with *p*-nitrophenyl phosphate (*p*NPP) or o-phenylenediamine hydrochloride (OPD) substrate (Sigma Chemical Co.). Optical densities (OD) were read using a Bio-Kinetics ELISA reader (BioTek Instruments, Winooski, VT, USA), and the respective concentrations of cytokines/chemokines were calculated based on the derived standard curve.

RNA silencing studies

SiRNA (small interfering RNA) was designed and prepared following established guidelines (*http://www.Ambion.com*), at the University of Texas Southwestern RNA Core Facility. The sequences of siRNA used for blocking *IRF-1* gene were 5′-GCC GAG ACA CUA AGA GCA ATT-3′, 5′-UUG CUC UUA GUG UCU CGG CTT-3′, 5′-UAC CAG AUA GCA CCA CUG ATT-3′, 5′-UCA GUG GUG CUA UCU GGU ATT-3′, 5′-UGG ACA GGA GUC AUC UUC UTT-3′, and 5′-AGA AGA UGA CUC CUG UCC ATT-3′. The control siRNA was a fluorescein isothiocyanate (FITC)-labeled scrambled oligonucleotide. SiRNA duplexes were made by annealing single-stranded siRNA. This was then added dropwise to the mesangial cells in culture, together with GeneEraser transfection reagent (Stratagene, La Jolla, CA, USA) at room temperature. After 10 minutes, the wells were washed, and fresh culture media was added. After 24 hours of culture, 10 ng/mL LPS was added for different durations. Transfection efficiency was gauged by FACS analysis.

Anti-GBM studies

GBM-reactive nephrotoxic serum was prepared as described elsewhere [4, 5]. B6 and B6.*IRF-1*$^{-/-}$ mice were purchased from Jackson Laboratories, and maintained in an SPF colony. Two- to three-month-old females were used for all studies. Nephrotoxic serum nephritis was induced as described previously [4, 5]. Briefly, mice were sensitized with rabbit IgG on day 0, and administered a single dose (150 ug per 25 mg body weight) of anti-GBM

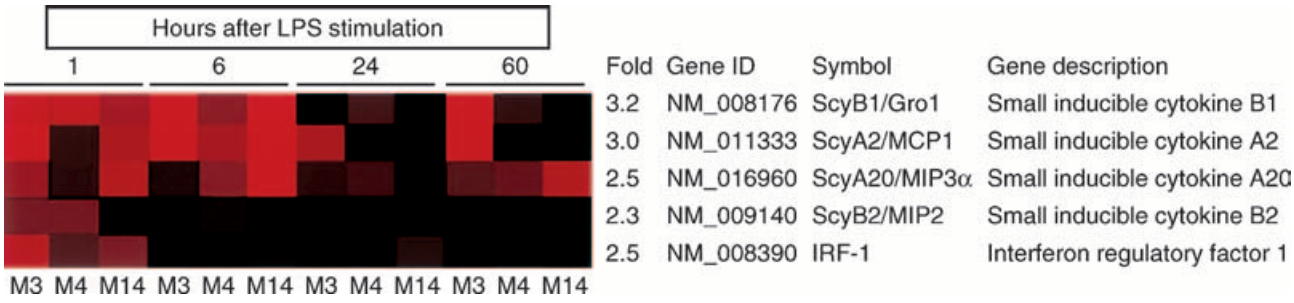

Fig. 1. Mesangial genes turned on 1 hour following lipopolysaccharide (LPS) stimulation. Mesangial cell lines were stimulated with 10 ng/mL LPS. RNA was extracted 0, 1, 6, 24, and 60 hours poststimulation. Whereas RNA from the unstimulated sample was cyanine-3 (Cy3) labeled, RNA from the stimulated cells was Cy5-labeled. Both sets of labeled RNA were then cohybridized to 17K oligonucleotide arrays and scanned. After filtering noise, the intensity in the Cy5 channel was compared to that in the Cy3 channel. Results from three biologic replicates (from three independent B6-derived mesangial lines, M3, M4, and M14) are presented in successive columns, under each timepoint. The expression patterns of genes that showed at least a twofold increase following LPS stimulation at the 1-hour time point are depicted. The indicated fold change pertains to the average fold increase observed in the three mesangial cell lines, at the 1-hour time point. The NCBI/Unigene ID, gene symbol, and gene description are also indicated.

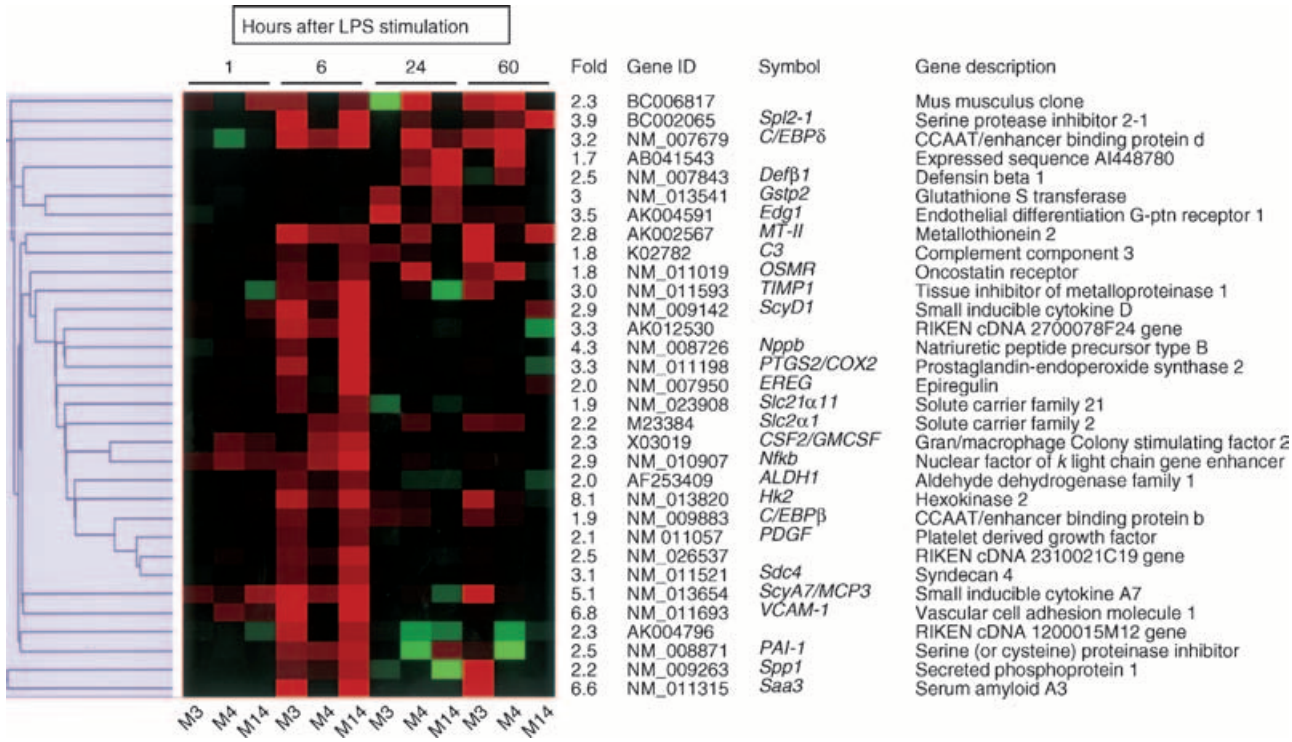

Fig. 2. Mesangial genes turned on 6 to 24 hours following lipopolysaccharide (LPS) stimulation. Three independent mesangial cell lines were stimulated with LPS, and studied as detailed in Figure 1. The expression patterns of genes that showed at least a twofold increase following LPS stimulation only at the 6- and/or 24-hour time points are depicted in this figure. The indicated fold change pertains to the average fold-increase observed in the three mesangial cell lines, at the 6-hour or 24-hour time point, whichever exhibited a larger fold increase. The NCBI/Unigene ID, gene symbol, and gene description are also indicated.

"nephrotoxic" sera on day 5. Mice were then monitored for evidence of disease on day 14. Urinary protein concentration was determined using the Coomassie Plus protein Assay Kit (Pierce, Rockford, IL, USA). Urine albumin concentration was assayed using a commercially available kit (Bethyl Laboratories, Montgomery, TX, USA). Blood was collected on day 0 and day 14, for measuring blood urea nitrogen (BUN), using a urea nitrogen kit (Sigma Chemical Co.).

Statistics

Intergroup comparisons (at the respective time points at which gene changes were noted) were carried out

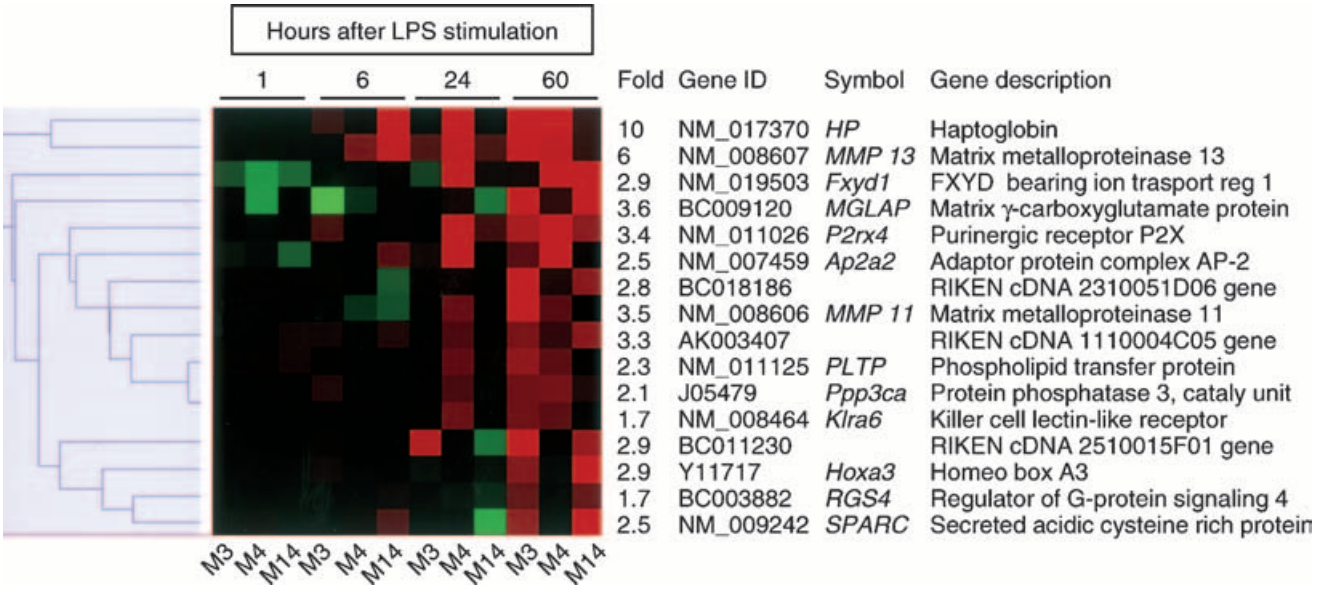

Fold	Gene ID	Symbol	Gene description
10	NM_017370	*HP*	Haptoglobin
6	NM_008607	*MMP 13*	Matrix metalloproteinase 13
2.9	NM_019503	*Fxyd1*	FXYD bearing ion trasport reg 1
3.6	BC009120	*MGLAP*	Matrix γ-carboxyglutamate protein
3.4	NM_011026	*P2rx4*	Purinergic receptor P2X
2.5	NM_007459	*Ap2a2*	Adaptor protein complex AP-2
2.8	BC018186		RIKEN cDNA 2310051D06 gene
3.5	NM_008606	*MMP 11*	Matrix metalloproteinase 11
3.3	AK003407		RIKEN cDNA 1110004C05 gene
2.3	NM_011125	*PLTP*	Phospholipid transfer protein
2.1	J05479	*Ppp3ca*	Protein phosphatase 3, cataly unit
1.7	NM_008464	*Klra6*	Killer cell lectin-like receptor
2.9	BC011230		RIKEN cDNA 2510015F01 gene
2.9	Y11717	*Hoxa3*	Homeo box A3
1.7	BC003882	*RGS4*	Regulator of G-protein signaling 4
2.5	NM_009242	*SPARC*	Secreted acidic cysteine rich protein

Fig. 3. Mesangial genes turned on 60 hours following lipopolysaccharide (LPS) stimulation. Three independent mesangial cell lines were stimulated with LPS, and studied as detailed in Figure 1. The expression patterns of genes that showed at least a twofold increase following LPS stimulation only at the 60-hour time point are depicted in this figure. The indicated fold change pertains to the average fold increase observed in the three mesangial cell lines, at the 60-hour time point. The NCBI/Unigene ID, gene symbol, and gene description are also indicated.

using analysis of variance (ANOVA), or the Student *t* test, unless otherwise indicated. All statistical analyses were performed using SigmaStat (Jandel Scientific).

RESULTS

Of the large array of genes monitored, a set of five genes demonstrated rapid and consistent up-regulation (> twofold) in mesangial cells, within an hour following LPS activation. These included *IRF-1* ($P < 0.02$), *ScyA2* (*MCP1*) ($P < 0.007$), *ScyA20 (MIP3α)* ($P < 0.04$), *ScyB1* (*Gro1*) ($P < 0.006$), and *ScyB2* (*MIP2α/Gro2*) ($P < 0.05$), as portrayed in Figure 1. Whereas the first is an interferon regulatory transcription factor, the rest are all chemokines. Whereas *IRF-1* and *ScyB2*/*MIP2α* were down-regulated back to resting levels by 6 hours poststimulation, *ScyA2*/*MCP1*, *ScyA20*/*MIP3α,* and *ScyB1/Gro1* continued to be expressed till at least 6 hours poststimulation; indeed, *ScyB1/Gro1* was expressed at least until 60 hours poststimulation, as is evident from Figure 1.

The mesangial transcriptomic profile 6 hours and 24 hours poststimulation with LPS were drastically different from the 1-hour profile, with heightened expression of a rich array of genes, belonging to many different functional groups, as illustrated in Figure 2. In addition to the continued expression of *ScyA2*/*MCP1*, *ScyA20*/*MIP3α(* and *ScyB1/Gro1* (Fig. 1), two additional chemokines became hyperexpressed, *ScyA7 (MCP3)* and *ScyD1* (fractalkine). Important growth factors that were up-regulated at this time point included *GM-CSF (CSF-2*), platelet-derived growth factor (*PDGF*) and *epiregulin* [belonging to the endothelial growth factor (EGF) family]. Several key transcription factors surfaced at this point, including nuclear factor-κB (*NFκB*), *C/EBP*β, and *C/EBP*δ. Of these transcription factors, *NFκB* appeared to be relatively early in its expression profile since it was modestly up-regulated as early as 1 hour post-LPS stimulation (albeit at levels that were < twofold), as is evident from Figure 2. Matrix remodeling enzymes, including *TIMP-1*, were also hyperexpressed at this time point. Inflammation-related molecules that became up-regulated included PTGS2/COX2, and several serine/cysteine proteinase inhibitors, including *SpI2-1*, *Spp1*, and plasminogen activated inhibitor-1 (*PAI-1*). Surface molecules that became up-regulated included vascular cell adhesion molecule-1 (*VCAM-1*) and *Syndecan-4.* complement factor *C3* and *defensin beta 1* up-regulation became prominent at the later, at the 24-hour time point. A suite of "metabolism"-related genes, including *Slc21a11*, *Slc2a1*, *ALDH1*, *glutathione*, *and hexokinase*, were also up-regulated at these intermediate (6 to 24 hours) time points. Finally, several novel genes of yet unknown function were also noted to be up-regulated.

The final microarray time point was at 60 hours post-LPS stimulation. Most of the genes that were up-regulated earlier had already been extinguished by this later time point, with a few exceptions, including *ScyB1/Gro1*, *C/EBP, oncostatin receptor, C3*, *CTLA2*, and *Saa3*, as can be noted from Figure 2. In addition, a set of new genes was turned on at this late time point, as diagramed in Figure 3. This included matrix-remodeling genes, including *MMP11*, *MMP13*, and *MGLAP*. In

Table 2. Genes that were down-regulated >twpfold, on the average

Gene ID	Time of maximal change	Average fold change	Gene symbol and description
Z37110	1 hour	−2.29	Ccng1, cyclin G1
AK018340	1 hour	−2.1	RIKEN cDNA 6530415H11 gene
NM_013493	24 hours	−3.87	Cnbp, cellular nucleic acid binding protein
NM_008947	24 hours	−3.62	Psmc1, protease
NM_013470	24 hours	−3.5	Anxa3, annexin A3
NM_025436	24 hours	−3.26	Sc4mol, sterol-C4-methyl oxidase-like
NM_019813	24 hours	−3.11	Dbn1, drebrin 1
NM_007840	24 hours	−2.89	Ddx5, DEAD
NM_008774	24 hours	−2.89	Pabpc1, poly A binding protein
NM_009790	24 hours	−2.8	Calm1, calmodulin 1
NM_008753	24 hours	−2.74	Oaz1, ornithine decarboxylase antizyme
NM_025323	24 hours	−2.74	RIKEN cDNA 0610009D07 gene
NM_008972	24 hours	−2.69	Ptma, prothymosin alpha
AK013880	24 hours	−2.68	Nars, asparaginyl-tRNA synthetase
NM_054044	24 hours	−2.66	RIKEN cDNA 9530074E10 gene
BC016232	24 hours	−2.55	Cappa1, capping protein alpha 1
AK011566	24 hours	−2.52	RIKEN cDNA 2610027H02 gene
NM_009795	24 hours	−2.5	Capns1, calpain
AK005460	24 hours	−2.49	Cnn3, calponin 3
NM_013556	24 hours	−2.46	Hprt, hypoxanthine guanine phosphoribosyl transferase
NM_013715	24 hours	−2.45	Cops5, COP9 (constitutive photomorphogenic) homolog
NM_011029	24 hours	−2.41	Lamr1, laminin receptor 1
BC005537	24 hours	−2.36	Hypothetical protein MGC7474
NM_025360	24 hours	−2.21	RIKEN cDNA 1200002G13 gene
NM_009082	24 hours	−2.2	Rpl29, ribosomal protein L29
NM_011292	24 hours	−2.2	Rbl9, ribosomal protein L9
NM_016786	24 hours	−2.18	Hip2, huntington interacting protein 2
NM_013562	24 hours	−2.16	Ifrd1, interferon-related developmental regulator 1
NM_019641	24 hours	−2.11	Stmn1, stathmin 1
NM_009658	24 hours	−2.1	Akrlb3, aldo-keto reductase family 1
NM_018865	24 hours	−2.08	Wisp1, WNT1-inducible signaling pathway protein 1
BC010215	24 hours	−2.04	Plekha2, pleckstrin homology domain-containing
AB029930	60 hours	−4.33	Cav, caveolin
NM_016750	60 hours	−3.08	H2A histone family
BC013552	60 hours	−2.84	Expressed sequence AU018965
AK013995	60 hours	−2.73	RIKEN cDNA 3110004O18 gene
NM_010634	60 hours	−2.32	Fabp5, fatty acid binding protein 5
BC010711	60 hours	−2.24	Mus, musculus cDNA clone
NM_020332	60 hours	−2.19	ank, progressive ankylosis
NM_008342	60 hours	−2.17	Igfbp2, insulin-like growth factor binding protein 2
L21027	60 hours	−2.14	Phgdh, 3-phosphoglycerate dehydrogenase
NM_013642	60 hours	−2.11	Dusp1, protein tyrosine phosphatase
BC021333	60 hours	−2.07	RIKEN cDNA 2610034E13 gene
BC008520	60 hours	−2	Vcl, vinculin

addition to genes being up-regulated, several genes were also down-regulated in LPS-triggered mesangial cells. Summarized in Table 2 are all genes that were down-regulated twofold or more in at least two of three mesangial cell lines studied. Very few genes showed maximal down-regulation at the 1-hour and 6-hour time points (Table 2), as opposed to the 24-hour time point. Finally, most of the genes down-regulated at the 24-hour time point also remained suppressed at the 60-hour time point.

To confirm the validity of the above microarray results, several of the up-regulated genes were selected for further confirmatory studies, using real-time RT-PCR assays, or ELISA. Shown in Figure 4 are the message up-regulation profiles of *IRF*-1 and *ScyB1/Gro1*, as ascertained by real-time PCR. As is clear from Figure 1 and Figure 4, whereas *IRF*-1 appeared to be a "quick-on, quick-off" gene, *ScyB1/Gro1* was rapidly turned on, but was persistently expressed. ELISA assays also offered confirmation of increased MCP-1 protein levels following LPS stimulation (Fig. 4E). Likewise, the data shown in Figure 5 validate several of the intermediate/late time point gene changes, including complement C3, GM-CSF/CSF2, TIMP-1, and MMP-13, using real-time PCR or ELISA. These confirmatory studies and supporting literature (see below), together lend credence to the validity of the transcriptomic findings portrayed in Figures 1 to 3.

From the above results, it was apparent that *IRF-1* was the earliest transcription factor to be hyperexpressed following LPS stimulation, with *NFκB* being a close second. Hence, we wondered if it might be a potential target for molecular intervention. Before attempting to test the function of this molecule in mesangial cells, we asked what other triggers were capable of up-regulating *IRF-1* expression. It became clear that several other innate

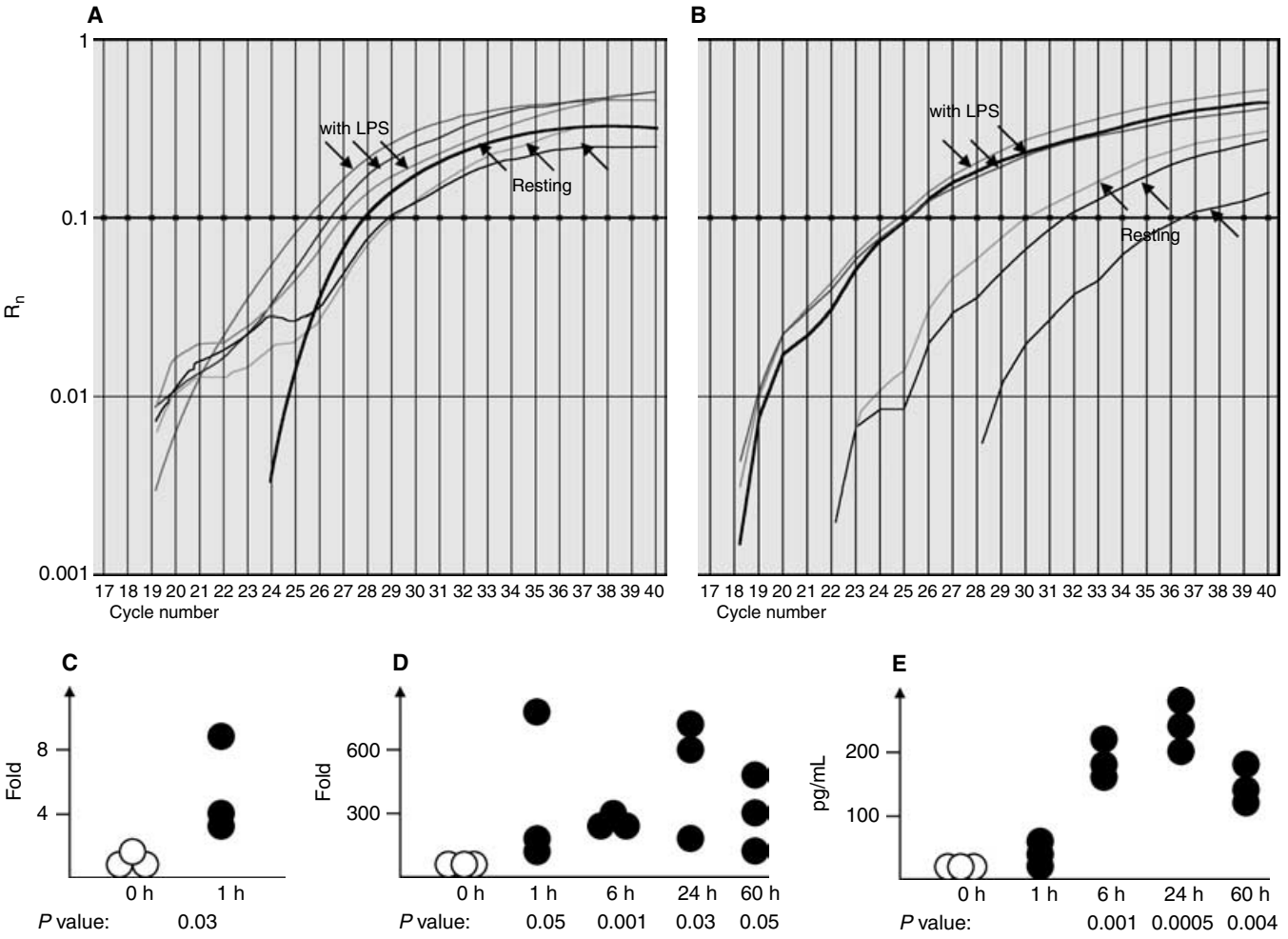

Fig. 4. Confirmation of expression profiles of "early-on" genes. To confirm the microarray results presented in Figure 1, the expression levels of interferon regulatory factor-1 (*IRF-1*) and *ScyB1/Gro*-1 were measured by real-time polymerase chain reaction (PCR). RNA isolated from unstimulated and lipopolysaccharide (LPS)-stimulated mesangial cells were reverse transcribed (RT), and PCR amplified over a spectrum of cycles. The cycle number that yielded a threshold level of PCR product was noted (C_T), and this was used to calculate the "fold increase" using the relative C_T method, after normalization against glyceraldehyde-3-phosphate dehydrogenase (*GAPDH*) (see **Methods** section). The *IRF-1* (*A*) and *Scy-B1/Gro-1* (*B*) PCR product levels are plotted as a function of PCR cycle number for three independent mesangial lines that were either unstimulated or LPS-stimulated for 1 hour. The same data are shown quantitatively in (*C*) and (*D*), respectively. Likewise, mesangial cell monocyte chemoattractant protein-1 (MCP-1) production after LPS stimulation was verified using enzyme-linked immunosorbent assay (ELISA) (*E*). Indicated *P* values pertain to Student *t* test comparisons of expression levels at "T = 0" versus the expression levels at various time points after LPS stimulation. Shown results are representative of two to three independent experiments, for each gene studied.

triggers (e.g., poly I:poly C and peptidoglycan), but not all, also had the potential to up-regulate *IRF-1* in mesangial cells (Fig. 6). In addition, INF-γ was one of the most potent triggers of *IRF-1* expression. Finally, heat-aggregated pooled IgG, a surrogate for immune complexes (triggering via FcR), also demonstrated the capacity to trigger mesangial cell *IRF-1* expression. Hence, *IRF-1* appeared to be an early gene turned on in mesangial cells, following several different types of triggers.

Given that *IRF-1* was one of the earliest transcription factors to be turned on following mesangial cell stimulation, we asked what role this molecule might be playing in the later appearing events. To ascertain this, *IRF-1* up-regulation was first suppressed using an *IRF-1* targeted siRNA construct (or placebo), before LPS stimulation. As is clear from Figure 7, successful expression of siRNA (as confirmed by flow cytometry) (Fig. 7A) reduced cellular levels of *IRF-1* effectively (Fig. 7B), but was not capable of dampening other downstream mediators following LPS stimulation (Fig. 7C). Whereas some of the assayed products have been shown to be transcriptionally controlled (Figs. 1 to 3), others have previously been documented to be major products of mesangial cells [1–3]. Somewhat surprised by these negative results, B6.*IRF-1*$^{-/-}$ mice were procured, and mesangial cell lines were isolated for study. As is evident from Figure 8A, mesangial cells from the knockout mice were equally capable of producing several downstream mediators following LPS

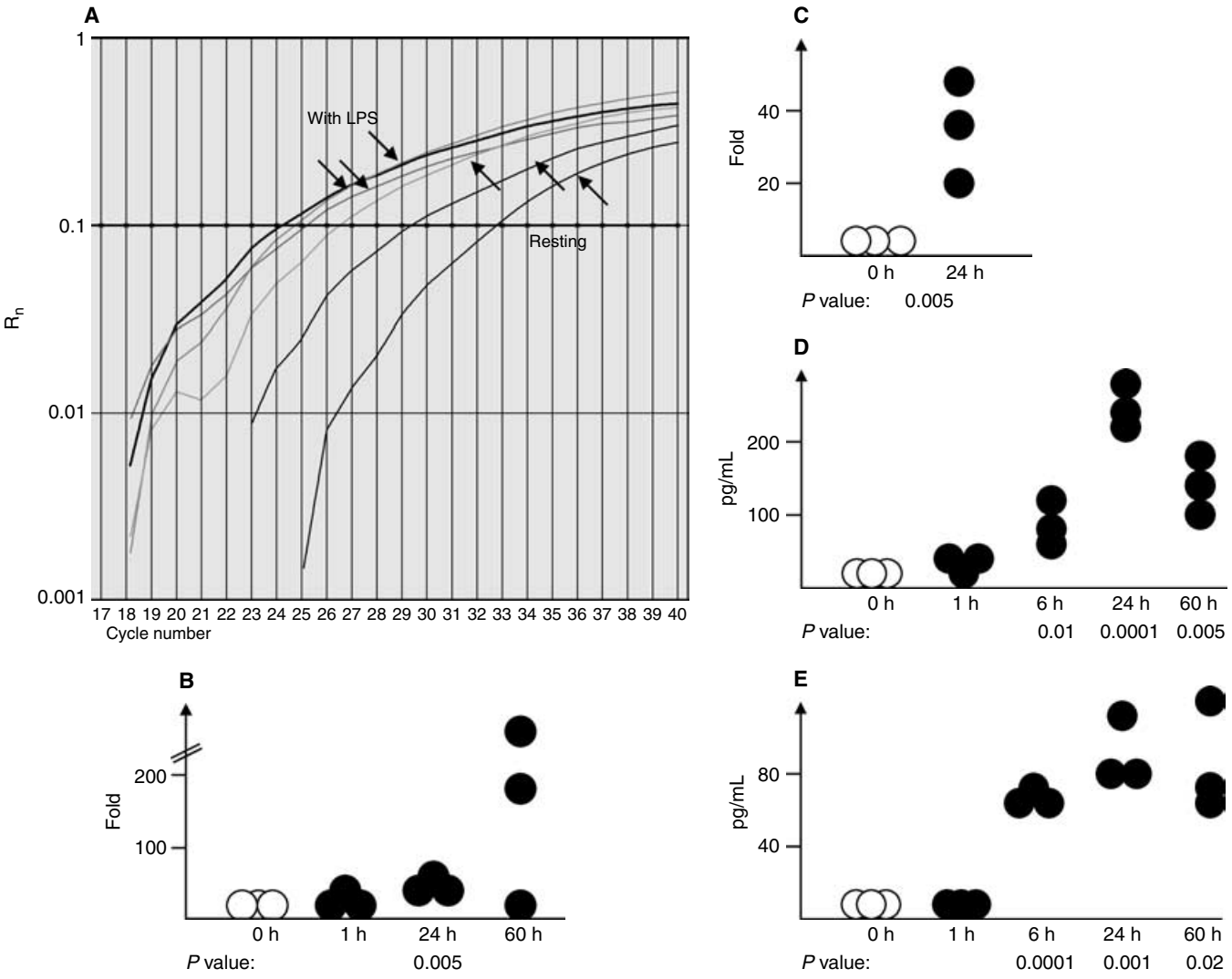

Fig. 5. Confirmation of expression profiles of "intermediate/late" time point genes. To confirm the microarray results presented in Figures 2 and 3, the expression of several genes were tested by real-time polymerase chain reaction (PCR) or enzyme-linked immunosorbent assay (ELISA). Complement component, *C3* (*A* and *B*), and *MMP13* (*C*) were measured by real-time PCR, and quantitated as detailed in the legend to Figure 4. PCR product levels for *C3* are plotted as a function of PCR cycle number, for three independent mesangial lines that were either unstimulated, or lipopolysaccharide (LPS)-stimulated for 24 hours (A and B), or for 60 hours (B). Likewise, mesangial cell tissue inhibitor metalloproteinase-1 (TIMP-1) (*D*) and granulocyte macrophage-colony-stimulating factor (GM-CSF)/CSF-2 (*E*) production after LPS stimulation were verified using ELISA. Each dot represents data obtained from an independent B6-derived mesangial cell line. Indicated *P* values pertain to Student *t* test comparisons of expression levels at "T = 0" versus the expression levels at various time points after LPS stimulation. Shown results are representative of two to three independent experiments, for each gene studied.

stimulation. In addition, when subjected to challenge with rabbit anti-GBM "nephrotoxic" sera, B6.*IRF-1*$^{-/-}$ mice suffered a similar extent of proteinuria (including albuminuria) and azotemia, as the B6 controls (Fig. 8B).

Finally, the hyperexpressed genes at the different time points were examined to determine if they shared any particular transcription factor binding sites. Although the 5 "early on" genes up-regulated 1-hour poststimulation did not significantly share any particular transcription factor binding sites, the "intermediate" and "late" appearing genes revealed interesting patterns, with respect to shared transcription factor binding sites. As portrayed in Figure 9, a substantial fraction of these genes exhibited canonical binding sites for C/EBP, NF-ATp, Sp1, and a couple of other transcription factors. Particularly prominent was the observation that nearly 70% of all intermediate and late LPS response genes exhibited Sp1 binding sites.

DISCUSSION

The above studies point to an ordered expression of several different classes of molecules in carefully synchronized waves, following LPS stimulation of mesangial

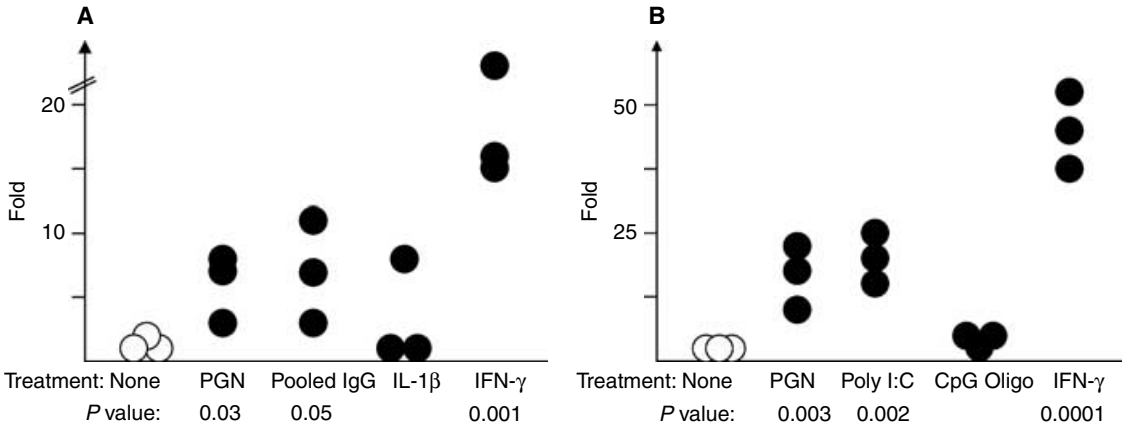

Fig. 6. Stimuli that trigger interferon regulatory factor-1 (*IRF-1*) expression in mesangial cells. (*A*) Three independent B6-derived mesangial cell lines (indicated as individual dots) were stimulated with a variety of stimuli, including peptidoglycan (PGN), heat-aggregated pooled rabbit IgG (pooled IgG), interleukin (IL)-1β, and interferon-γ (IFN-γ), at doses detailed in the **Methods** section. *IRF-1* expression was measured 1 hour after stimulation, by real-time polymerase chain reaction (PCR). Depicted *P* values pertain to Student *t* test comparison of *IRF-1* levels after stimulation, against the resting level of *IRF-1* message in unstimulated cells. (*B*) In the second experiment, one of the three B6-derived mesangial cell lines was cultured in triplicate (indicated as individual dots), and stimulated with a variety of stimuli, including PGN, poly I:polyC, CpG oligonucleotides, and INF-γ, at doses detailed in the **Methods** section *IRF-1* expression was measured 1 hour after stimulation, by real-time PCR. Depicted *P* values pertain to Student *t* test comparison of *IRF-1* level after stimulation, against the resting message level of *IRF-1* in unstimulated cells. CpG, cytosine phosphate guanosine.

cells. Although there were no previous reports of mesangial transcriptomes against which the present findings can be compared, a rich literature exists on the transcriptomes of macrophages, which are related to mesangial cells in ontogeny. Importantly, with respect to the "early-on" genes depicted in Figure 1, microarray studies using mouse and human macrophages have reported the early up-regulation of *ScyB2/MIP2α* [7–16], *IRF-1* [7–10, 12–15], *ScyA2/MCP-1* [7, 9, 12, 14, 15], and *ScyB1/Gro1* [7, 16], following a variety of stimuli, including innate triggers, infection, cytokines, and even physical triggers.

Although we do not have access to a rich literature on mesangial transcriptomes, several of the above molecules have been noted to be up-regulated in mesangial cells, following stimulation with LPS or other triggers. Notably, a large body of literature has detailed the up-regulation of *ScyA2/MCP-1* in stimulated mesangial cells [1–3, 17–19]; indeed, the critical in vivo role of this molecule in immune nephritis has also been demonstrated using *ScyA2/MCP-1* knockout mice [20]. In addition, a handful of reports have described the up-regulation of the other chemokines in mesangial cells, in resonance with the findings reported here [1–3, 17–21]. Collectively, the above studies in macrophages and mesangial cells further validate the observed changes in the present microarray study.

With respect to the transcription factors that were hyperexpressed, *IRF-1* and *NFκB* were the earliest to be up-regulated, though only the former was expressed in excess of twofold at the 1-hour time point. The role of *NFκB* in mesangial cell stimulation has previously been demonstrated [22–24]. The present communication evaluates the potential importance of the other early transcription factor, *IRF-1*. Although the literature on mesangial *IRF-1* is rather limited, this is a well-studied molecule in other cell models. Indeed, both *IRF-1* and *NFκB* exhibit transcriptional synergy as they come together to generate "enhancesomes," which also include other factors such as activating transcription factor (ATF)-2/c-Jun and 3-hydroxy-3-methylglutaryl (HMG)-I [25, 26]. Importantly, *IRF-1* has been documented in the transcriptional control of many genes, including *type I IFN* [27], *MMPs* [28], *VCAM-1* [29], and *COX-2* [30], several of which have been noted to be up-regulated in the present study (Figs. 2 and 3).

This is also the first documentation of *IRF-1* up-regulation in mesangial cells following a wide spectrum of triggers, innate or otherwise. It is known that mesangial cells can be triggered via FcR [31, 32], and the present communication highlights *IRF-1* expression as an early consequence of this signaling (Fig. 7). Given that *IRF-1* is an early transcriptional regulator in mesangial cells following a wide spectrum of triggers, it seemed to be an attractive target for modulation. Surprisingly, the deliberately blocking *IRF-1,* as well as the genetic deficiency of *IRF-1,* both failed to subdue the expression of key downstream molecules (Figs. 7 and 8). It is possible that *IRF-1* may be redundant, or unnecessary for the biologic responses being examined in this communication, with respect to the role of particular in vitro and in vivo stimuli used. In this respect, for example, the biological relevance of *IRF-1* has largely been demonstrated in response to INF stimulation [28 30, 33].

Moreover, the optimal firing of downstream pathways in mesangial cells may be contingent upon synergy between several different transcriptional factors,

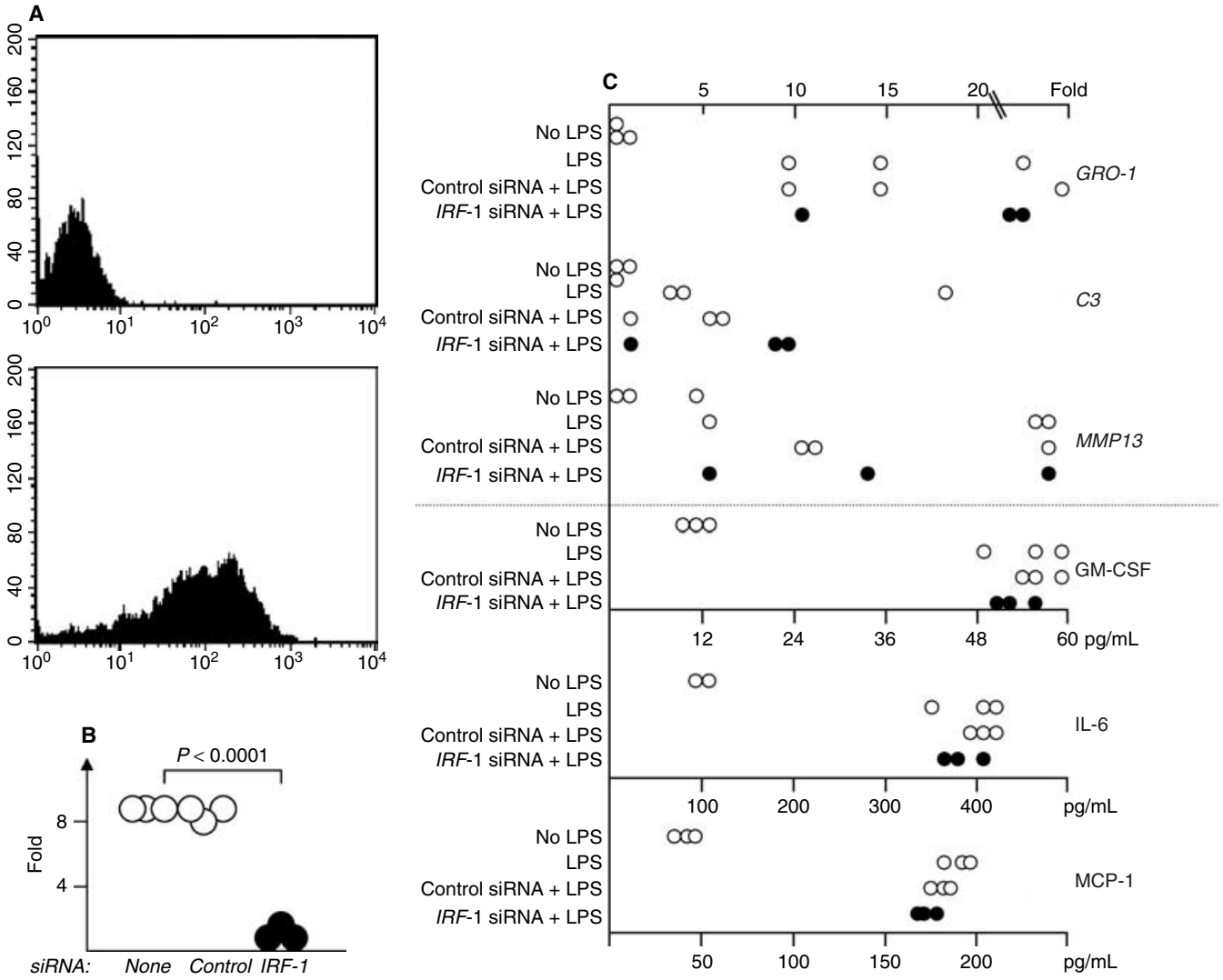

Fig. 7. Evaluating the role of interferon regulatory factor-1 (*IRF-1*) in mesangial cell function. (*A*) The FACS profiles of mesangial cells stained to reveal the uptake of fluorescein isothiocyanate (FITC)-labeled small interfering RNA (siRNA). The plot on the bottom shows the uptake of labeled siRNA. Use of siRNA targeted to *IRF-1* dampened *IRF-1* message levels, as expected (*B*), but not those of several other molecules assayed (*C*), by real-time reverse transcription-polymerase chain reaction (RT-PCR) or enzyme-linked immunosorbent assay (ELISA). For the real-time PCR assays, fold change was calculated as described in the legend to Figure 4. Each dot represents data obtained from one of three independent mesangial cell lines. Shown data are representative of two independent experiments, with similar results.

including *NFκB* and *IRF-1*, *C/EBP*, etc. [25, 26, 33], all of which were up-regulated in LPS-triggered mesangial cells (Fig. 2). In addition, the mesangial cell response following LPS stimulation may also be programmed by yet other transcription factors such as Sp1, and NFAT-p, as revealed by the computer-based search against the publicly accessible transcription factor database (Fig. 9). Indeed, the roles of several of these transcription factors in endotoxin-triggered biologic responses have been richly documented in other cell systems [34–40]. It remains to be shown if any of these factors play an obligatory role in mesangial cell response to LPS stimulation.

LPS has been widely used as an in vitro trigger for a large number of cell types, including mesangial cells. Indeed, when coadministered with organ-specific autoantibodies (e.g., anticollagen or antiglomerular antibodies), it has been observed to precipitate profound end organ disease. Hence, it has turned out to be an excellent experimental tool for studying cellular function in vitro and end-organ disease in vivo. On the other hand, one may ask if the use of LPS as a trigger has any biologic relevance. Given that LPS stimulates cellular processes via Toll receptors, and the recent observation that an increasing number of self-molecules (e.g., heat shock proteins, fibronectin) can also trigger the same toll receptors [41–42], it is attractive to posit that some of these endogenous ligands may have the potential to impact the very same biologic pathways influenced by LPS. Identifying the

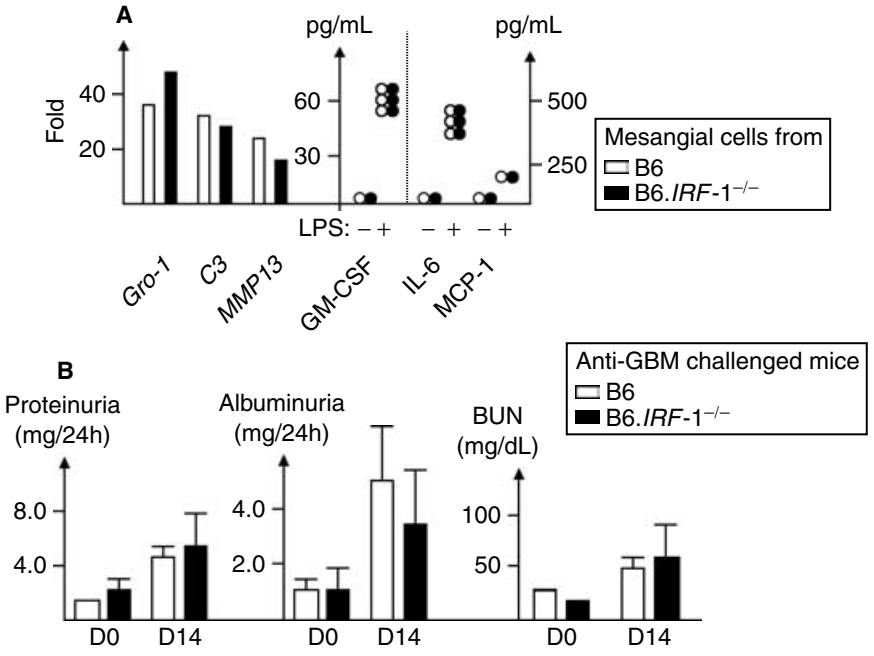

Fig. 8. Impact of interferon regulatory factor-1 (*IRF-1*) deficiency on mesangial cell function and anti-glomerular basement membrane (GBM) disease. (*A*) Mesangial cells derived from B6 (open circles or bars) and B6.*IRF-1*$^{-/-}$ (closed circles or bars) were stimulated with lipopolysaccharide (LPS) (10 ng/mL) and assayed for various downstream mediators. Whereas complement *C3, Gro-1,* and maxtrix metalloproteinase-13 (*MMP13*) were assayed by real-time polymerase chain reaction (PCR), the other mediators were measured using enzyme-linked immunosorbent assay (ELISA). For the real-time PCR assays, each bar represents the mean expression level in triplicate cultures, 1 hour after LPS stimulation. For the ELISA assays, results from triplicate cultures are shown; where the values overlapped, this is represented with single dots only. No significant differences were noted in the expression levels of any of the molecules studied. Both the real-time PCR and ELISA assays shown are representative of two repeat experiments each, with similar findings. (*B*) B6.*IRF-1*$^{-/-}$ mice and B6 controls were challenged with rabbit anti-GBM sera, and monitored for disease over a period of 14 days, as detailed in the Methods section. Shown are the 24-hour urine protein content, albumin content, and blood urea nitrogen (BUN) levels on day 0 and day 14 in the two strains studied (N = 5 mice per group). The mean ± SEM values are shown, and the differences observed were not statistically significant.

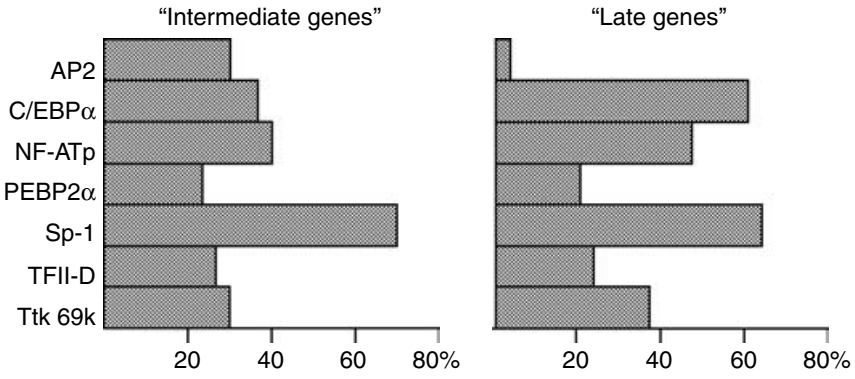

Fig. 9. Transcription factor binding sites in differentially expressed genes. All genes that were differentially expressed were examined for transcription factor binding sites in their 5′ untranslated regions, as detailed in the **Methods** section. Among the genes that were hyper-expressed between 6 and 24 hours, and among those that were hyperexpressed at 60 hours, several were found to share transcription factor binding sites. Displayed are the seven most commonly present transcription factor binding sites in the 5′ regulatory regions of these genes.

endogenous ligands within the glomerular milieu that may potentially engage toll receptors on mesangial cells is a challenge that lies ahead.

ACKNOWLEDGMENTS

This work is funded in part by grants from the NIH (R01 AR50812 and PO1 AI39824), and the National Arthritis Foundation.

Reprint requests to Chandra Mohan, M.D., Ph.D., Simmons Arthritis Research Center, Department of Internal Medicine/Rheumatology University of Texas Southwestern Medical Center, Mail Code 8884, Y8.204, 5323 Harry Hines Boulevard, Dallas, TX 75390–8884.
E-mail: Chandra.mohan@utsouthwestern.edu

REFERENCES

1. Veis JH, Yamashita W, Liu YJ, Ooi BS: The biology of mesangial cells in glomerulonephritis. *Proc Soc Exp Biol Med* 195:160–167, 1990
2. Hawkins NJ, Wakefield D, Charlesworth JA: The role of mesangial cells in glomerular pathology. *Pathology* 22:24–32, 1990
3. Radeke HH, Resch K: The inflammatory function of renal glomerular mesangial cells and their interaction with the cellular immune system. *Clin Investigator* 70:825–842, 1992
4. Xie C, Zhou XJ, Liu X, Mohan C: Enhanced intrinsic susceptibility to renal disease in the lupus facilitating NZW strain. *Arthritis Rheum* 48:1080–1092, 2003
5. Xie C, Sharma R, Wang H, *et al*: Strain distribution pattern of susceptibility to immune-mediated nephritis. *J Immunol* 172:5047–5055, 2004

6. Striker GE, Striker LJ: Glomerular cell culture. *Lab Invest* 53:122–131, 1985
7. Lang R, Patel D, Morris JJ, *et al*: Shaping gene expression in activated and resting primary macrophages by IL-10. *J Immunol* 169:2253–2263, 2002
8. Scott MG, Rosenberger CM, Gold MR, *et al*: An alpha-helical cationic antimicrobial peptide selectively modulates macrophage responses to lipopolysaccharide and directly alters macrophage gene expression. *J Immunol* 165:3358–3365, 2000
9. Nau GJ, Richmond JF, Schlesinger A, *et al*: Human macrophage activation programs induced by bacterial pathogens. *Proc Natl Acad Sci USA* 99:1503–1508, 2002
10. Greenwell-Wild T, Vazquez N, Sim D, *et al*: Mycobacterium avium infection and modulation of human macrophage gene expression. *J Immunol* 169:6286–6297, 2002
11. Eskra L, Mathison A, Splitter G: Microarray analysis of mRNA levels from RAW264.7 macrophages infected with Brucella abortus. *Infect Immunol* 71:1125–1133, 2003
12. Frenkel O, Shani E, Ben-Bassat I, *et al*: Activated macrophages for treating skin ulceration: Gene expression in human monocytes after hypo-osmotic shock. *Clin Exp Immunol* 128:59–66, 2002
13. Buates S, Matlashewski G: Identification of genes induced by a macrophage activator, S-28463, using gene expression array analysis. *Antimicrob Agents Chemother* 45:1137–1142, 2001
14. Nakachi N, Matsunaga K, Klein TW, *et al*: Differential effects of virulent versus avirulent *Legionella pneumophila* on chemokine gene expression in murine alveolar macrophages determined by cDNA expression array technique. *Infect Immunol* 68:6069–6072, 2000
15. Rosenberger CM, Scott MG, Gold MR, *et al*: Salmonella typhimurium infection and lipopolysaccharide stimulation induce similar changes in macrophage gene expression. *J Immunol* 164:5894–5904, 2000
16. Detweiler CS, Cunanan DB, Falkow S: Host microarray analysis reveals a role for the Salmonella response regulator phoP in human macrophage cell death. *Proc Natl Acad Sci USA* 98:5850–5855, 2001
17. Anders HJ, Vielhauer V, Kretzler M, *et al*: Chemokine and chemokine receptor expression during initiation and resolution of immune complex glomerulonephritis. *J Am Soc Nephrol* 12:919–931, 2001
18. Banas B, Luckow B, Moller M, *et al*: Chemokine and chemokine receptor expression in a novel human mesangial cell line. *J Am Soc Nephrol* 10:2314–2322, 1999
19. Grande JP, Jones ML, Swenson CL, *et al*: Lipopolysaccharide induces monocyte chemoattractant protein production by rat mesangial cells. *Lab Clin Med* 124:112–117, 1994
20. Tesch GH, Schwarting A, Kinoshita K, *et al*: Monocyte chemoattractant protein-1 promotes macrophage-mediated tubular injury, but not glomerular injury, in nephrotoxic serum nephritis. *J Clin Invest* 103:73, 1999
21. Wu X, Dolecki GJ, Lefkowith JB: GRO chemokines: A transduction, integration, and amplification mechanism in acute renal inflammation. *Am J Physiol*. 269:F248–F256, 1995
22. Guijarro C, Kim Y, Kasiske BL, *et al*: Central role of the transcription factor nuclear factor-kappa B in mesangial cell production of chemokines. *Contrib Nephrol* 120:210–218, 1997
23. Rovin BH, Dickerson JA, Tan LC, *et al*: Activation of nuclear factor-kappa B correlates with MCP-1 expression by human mesangial cells. *Kidney Int* 48:1263–1271, 1995
24. Lopez-Franco O, Suzuki Y, Sanjuan G, *et al*: Nuclear factor-kappa B inhibitors as potential novel anti-inflammatory agents for the treatment of immune glomerulonephritis. *Am J Pathol* 161:1497–1505, 2002
25. Merika M, Williams AJ, Chen G, *et al*: Recruitment of CBP/p300 by the IFN beta enhanceosome is required for synergistic activation of transcription. *Mol Cell* 1:277–287, 1998
26. Saura M, Zaragoza C, Bao C, *et al*: Interaction of interferon regulatory factor-1 and nuclear factor kappaB during activation of inducible nitric oxide synthase transcription. *J Mol Biol* 289:459, 1999
27. Miyamoto M, Fujita T, Kimura Y, *et al*: Regulated expression of a gene encoding a nuclear factor, IRF-1, that specifically binds to IFN-beta gene regulatory elements. *Cell* 54:903–913, 1988
28. Sanceau J, Boyd DD, Seiki M, Bauvois B: Interferons inhibit tumor necrosis factor-alpha-mediated matrix metalloproteinase-9 activation via interferon regulatory factor-1 binding competition with NF-kappa B. *Biol Chem* 277:35766–35775, 2002
29. Ochi H, Masuda J, Gimbrone MA: Hyperosmotic stimuli inhibit VCAM-1 expression in cultured endothelial cells via effects on interferon regulatory factor-1 expression and activity. *Eur J Immunol* 32:1821–1831, 2002
30. Blanco JC, Contursi C, Salkowski CA, *et al*: Interferon regulatory factor (IRF)-1 and IRF-2 regulate interferon gamma-dependent cyclooxygenase 2 expression. *J Exp Med* 191:2131, 2000
31. Radeke HH, Janssen-Graalfs I, Sowa EN, *et al*: Opposite regulation of type II and III receptors for immunoglobulin G in mouse glomerular mesangial cells and in the induction of anti-glomerular basement membrane (GBM) nephritis. *J Biol Chem* 277:27535–27544, 2002
32. Hora K, Satriano JA, Santiago A, *et al*: Receptors for IgG complexes activate synthesis of monocyte chemoattractant peptide 1 and colony-stimulating factor 1. *Proc Natl Acad Sci USA* 89:1745–1749, 1992
33. Hurgin V, Novick D, Rubinstein M: The promoter of IL-18 binding protein: Activation by an IFN-gamma -induced complex of IFN regulatory factor 1 and CCAAT/enhancer binding protein beta. *Proc Natl Acad Sci USA* 99:16957–16962, 2002
34. Oeth P, Parry GC, Mackman N: Regulation of the tissue factor gene in human monocytic cells. Role of AP-1, NF-kappa B/Rel, and Sp1 proteins in uninduced and lipopolysaccharide-induced expression. *Arteriosclerosis, Throm Vasc Biol* 17:365–374, 1997
35. Ye X, Liu SF: Lipopolysaccharide regulates constitutive and inducible transcription factor activities differentially in vivo in the rat. *Biochem Biophys Res Comm* 288:927–932, 2001
36. Sakuta T, Matsushita K, Yamaguchi N, *et al*: Enhanced production of vascular endothelial growth factor by human monocytic cells stimulated with endotoxin through transcription factor SP-1. *J Med Microbiol* 50:233–237, 2001
37. Brightbill HD, Plevy SE, Modlin RL, *et al*: A prominent role for Sp1 during lipopolysaccharide-mediated induction of the IL-10 promoter in macrophages. *J Immunol* 164:1940–1951, 2000
38. Hu HM, Tian Q, Baer M, *et al*: The C/EBP bZIP domain can mediate lipopolysaccharide induction of the proinflammatory cytokines interleukin-6 and monocyte chemoattractant protein-1. *J Biol Chem* 275:16373–16381, 2000
39. Bradley MN, Zhou L, Smale ST: C/EBPbeta regulation in lipopolysaccharide-stimulated macrophages. *Mol Cell Biol* 23:4841–4858, 2003
40. Tengku-Muhammad TS, Hughes TR, Ranki H, *et al*: Differential regulation of macrophage CCAAT-enhancer binding protein isoforms by lipopolysaccharide and cytokines. *Cytokine* 12:1430–1436, 2000
41. Tsan M-F, Gao B: Endogenous ligands of Toll-like receptors. *J Leuko Biol* (online publication, 10.1189/jlb.0304127, April 30, 2004)
42. Beg AA: Endogenous ligands of Toll-like receptors: Implications for regulating inflammatory and immune responses. *Trends Immunol* 23:509–512, 2002